

Quantum measurement of hyperfine interaction in nitrogen-vacancy center

Kilhyun Bang, Wen Yang,* and L. J. Sham

Center for Advanced Nanoscience, Department of Physics,
University of California San Diego, La Jolla, California 92093-0319, USA

We propose an efficient quantum measurement protocol for the hyperfine interaction between the electron spin and the ^{15}N nuclear spin of a diamond nitrogen-vacancy center. In this protocol, a sequence of quantum operations of successively increasing duration is utilized to estimate the hyperfine interaction with successively higher precision approaching the quantum metrology limit. This protocol does not need the preparation of the nuclear spin state. In the presence of realistic operation errors and electron spin decoherence, the overall precision of our protocol still surpasses the standard quantum limit.

I. INTRODUCTION

The negatively charged nitrogen-vacancy (NV) center in diamond is a promising solid state system for quantum computation. The electron spin in the optical ground state of the NV center exhibits exceptionally long coherence time ($> 350 \mu\text{s}$) at room temperature.¹ This feature allows coherent manipulation and reliable readout of the state of the electron spin and the neighboring nuclear spins^{2,3} in the NV center, a key technique of diamond-based quantum computation.^{1,3-5} In these operations, the hyperfine interaction between the electron spin and the neighboring nitrogen nuclear spin plays an important role. To minimize the operation errors, an accurate estimate of the hyperfine interaction is desirable.

In addition to quantum computation, the NV center is also a candidate for the application of quantum parameter estimation (also known as quantum metrology). Quantum metrology seeks quantum measurement protocols to estimate physical parameters up to a given precision defined as $1/\Delta^2$ (with Δ being the standard deviation) using the least amount R of resources, which include the number of measurements, the total duration of the measurements, and the number of particles involved in the measurements. The classical protocol utilizes the number R of repeated measurements as a resource and, according to the central limit theorem, gives the classical limit (also known as standard quantum limit or SQL) $\Delta_{\text{SQL}} = O(1/\sqrt{R})$. Quantum metrology aims to surpass the SQL and, more ambitiously, reach the quantum metrology limit (QML) $\Delta_{\text{QML}} = O(1/R)$, the upper precision bound $1/\Delta_{\text{QML}}^2 = O(R^2)$ set by quantum mechanics. The most popular quantum measurement technique is interferometry, in which the parameter to be measured is recorded as a phase in the coherence of the system.⁶⁻⁹ The exceptionally long coherence time of the NV center electron spin diminishes the detrimental effect of decoherence on such measurements and makes the NV center an ideal system for quantum metrology.¹⁰ Up to date, most of the measurement protocols utilize pure quantum states and surpass the SQL by creating quantum entanglement in the system. However, the thermal equilibrium state of the nuclear spins is highly mixed at room temperature. To estimate *reliably* the hyperfine interaction in the NV center by a pure-state protocol, the nuclear spins must be prepared repeatedly into a given pure state. Further, the number of spins as the resources of entanglement in a single NV center is finite,⁵ so the advantage of quantum entanglement to parameter estimation is also

limited.

Recently, Boixo and Somma¹¹ proposed a model of mixed-state quantum metrology by combining the mixed-state quantum computation (also known as deterministic quantum computation with one quantum bit¹² or DQC1) with the adaptive Bayesian inference. This DQC1 model utilizes the total duration T (instead of large-scale entanglement¹⁰) of the estimation process as a resource to approach the QML $\Delta_{\text{QML}} = O(1/T)$ without creating any entanglement.^{13,14} However, its application to estimate the hyperfine interaction in the NV center requires including the effects of noise and unintended dynamics.

In this paper, we construct an efficient quantum measurement protocol to estimate the hyperfine interaction between the electron spin and the ^{15}N nuclear spin in the NV center. This protocol is essentially a combination of the DQC1 model¹¹ and the spin-echo technique,¹⁵ which decouples the dynamics driven by the hyperfine interaction from the noise and unintended dynamics. It does not need the preparation of the nuclear spin state and approaches the QML $\Delta_{\text{QML}} = O(1/T)$ in the ideal case. By including realistic errors (such as the nuclear spin rotation error and the electron spin decoherence) in our analysis, we show that our protocol still surpasses the SQL under typical experimental conditions.

The rest of this paper is organized as follows. In Sec. II, we review the DQC1 model for parameter estimation and identify the problems in applying this model to estimate the hyperfine interaction in the NV center. In Sec. III, we give a solution to these problems by combining the DQC1 model with the spin-echo technique. In Sec. IV, we introduce our quantum measurement protocol. Sec. V gives the conclusion.

II. DQC1 PARAMETER ESTIMATION IN NV CENTER

We first review the two-qubit version of the DQC1 parameter estimation model proposed by Boixo and Somma¹¹ (Sec. II A) and then identify the robustness problems arising from applying this model to estimate the hyperfine interaction in the NV center (Sec. II B).

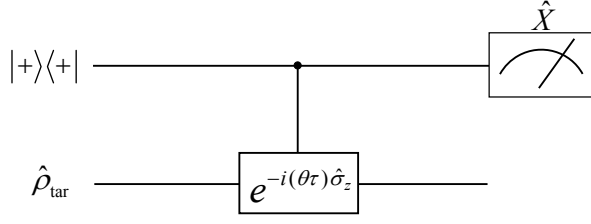


FIG. 1. DQC1 parameter estimation with one control qubit in the pure state $|+\rangle \equiv (|0\rangle + |1\rangle)/\sqrt{2}$ and one target qubit in the state $\hat{\rho}_{\text{tar}}$.

A. Two-qubit DQC1 parameter estimation

The two-qubit DQC1 model consists of a control qubit (with states $\{|0\rangle, |1\rangle\}$) and a target qubit (with states $\{|\uparrow\rangle, |\downarrow\rangle\}$). The initial state $\hat{\rho}_{\text{DQC1}} = |+\rangle\langle+| \otimes \hat{\rho}_{\text{tar}}$ is the direct product of the pure state $|+\rangle \equiv (|0\rangle + |1\rangle)/\sqrt{2}$ of the control qubit and the unpolarized state $\hat{\rho}_{\text{tar}} = (|\uparrow\rangle\langle\uparrow| + |\downarrow\rangle\langle\downarrow|)/2$ of the target qubit, as shown in Fig. 1. The three Pauli operators of the control qubit and of the target qubit are denoted by

$$\begin{aligned}\hat{X} &\equiv |1\rangle\langle 0| + |0\rangle\langle 1|, \\ \hat{Y} &\equiv i(|1\rangle\langle 0| - |0\rangle\langle 1|), \\ \hat{Z} &\equiv |0\rangle\langle 0| - |1\rangle\langle 1|,\end{aligned}$$

and $\{\hat{\sigma}_x, \hat{\sigma}_y, \hat{\sigma}_z\}$, respectively. The two qubits are coupled by the interaction

$$\hat{H}_{\text{DQC1}} = |1\rangle\langle 1| \otimes \theta \hat{\sigma}_z. \quad (1)$$

This interaction makes the splitting energy ω_c of the control qubit dependent on the state of the target qubit: $\omega_{c,\uparrow} = \theta$ for the target qubit in the spin-up state $|\uparrow\rangle$ and $\omega_{c,\downarrow} = -\theta$ for the target qubit in the spin-down state $|\downarrow\rangle$. The DQC1 parameter estimation¹¹ aims to estimate the interaction strength θ with the standard deviation $\Delta_\theta = O(1/T)$ approaching the QML, where T is the total duration of the estimation process. The procedures are simple: the application of the two-qubit interaction \hat{H}_{DQC1} for a duration τ , followed by a measurement of \hat{X} :

- If the target qubit is in the spin-up state $|\uparrow\rangle$, then \hat{H}_{DQC1} drives the precession of the control qubit with angular frequency $\omega_{c,\uparrow}$,

$$\frac{|0\rangle + |1\rangle}{\sqrt{2}} \otimes |\uparrow\rangle \rightarrow \frac{|0\rangle + e^{-i\omega_{c,\uparrow}\tau} |1\rangle}{\sqrt{2}} \otimes |\uparrow\rangle.$$

Before the measurement, the interaction strength θ is encoded as a phase $e^{-i\omega_{c,\uparrow}\tau}$ of the control qubit. The repeated measurements of \hat{X} estimate the average value $\langle \hat{X} \rangle_\uparrow = \cos(\omega_{c,\uparrow}\tau) = \cos(\theta\tau)$, which yields the phase.

- If the target qubit is in the spin-down state $|\downarrow\rangle$, then \hat{H}_{DQC1} drives the precession of the control qubit with angular frequency $\omega_{c,\downarrow}$,

$$\frac{|0\rangle + |1\rangle}{\sqrt{2}} \otimes |\downarrow\rangle \rightarrow \frac{|0\rangle + e^{-i\omega_{c,\downarrow}\tau} |1\rangle}{\sqrt{2}} \otimes |\downarrow\rangle.$$

Before the measurement, the interaction strength θ is encoded as a phase $e^{-i\omega_{c,\downarrow}\tau}$ of the control qubit. The repeated measurements of \hat{X} estimate the average value $\langle \hat{X} \rangle_\downarrow = \cos(\omega_{c,\downarrow}\tau) = \cos(\theta\tau)$, which extracts the phase.

- Now the target qubit is in the unpolarized state, i.e., an equal, incoherent mixture of $|\uparrow\rangle$ and $|\downarrow\rangle$. Then the repeated measurements of \hat{X} estimates the equally weighted average of $\langle \hat{X} \rangle_\uparrow$ and $\langle \hat{X} \rangle_\downarrow$:

$$\langle \hat{X} \rangle = \frac{1}{2}(\langle \hat{X} \rangle_\uparrow + \langle \hat{X} \rangle_\downarrow) = \cos(\theta\tau).$$

A distinctive feature of the above parameter estimation process is the absence of any two-qubit entanglement.¹⁴

For a given standard deviation $\Delta_X (\ll 1$ under typical situations) in estimating $\langle \hat{X} \rangle$, the DQC1 model gives an estimate to the interaction strength θ with a standard deviation

$$\Delta_\theta = \frac{\Delta_X}{|\partial \langle \hat{X} \rangle / \partial \theta|} = \frac{\Delta_X}{\tau |\sin(\theta\tau)|} \geq \frac{\Delta_X}{\tau}. \quad (2)$$

By regarding the duration τ of the estimation as a resource, the QML scaling $\Delta_\theta = O(1/\tau)$ is achieved if τ could be chosen such that $|\sin(\theta\tau)| \approx 1$. However, due to the limited prior knowledge about θ (the parameter to be estimated), we cannot always ensure $|\sin(\theta\tau)| \approx 1$, especially when a small standard deviation $\Delta_\theta \rightarrow 0$ (corresponding to large $\tau \rightarrow \infty$) is required.

To address this issue, Boixo and Somma¹¹ quantified the prior knowledge about θ by a standard deviation Δ_0 and utilized the adaptive Bayesian inference to reduce the standard deviation successively. The essential idea of this approach can be understood *qualitatively* as follows. In order to ensure $|\sin(\theta\tau)| \approx 1$ and hence the QML, the largest τ is roughly $1/\Delta_0$. Under this restriction, the minimal standard deviation for the estimation of θ is given by Eq. (2) as $\sim \Delta_X \Delta_0 \ll \Delta_0$. Therefore, the DQC1 measurements with standard deviation Δ_X refines our knowledge about the interaction strength θ from a large standard deviation Δ_0 to a much smaller one $\sim \Delta_X \Delta_0$. By iterating this procedure, the standard deviation Δ_θ would decrease successively as $\Delta_0 \rightarrow \Delta_X \Delta_0 \rightarrow \Delta_X^2 \Delta_0 \rightarrow \dots$. With the aid of the adaptive Bayesian inference, Boixo and Somma¹¹ performed a quantitative analysis about this iteration and concluded that the QML $\Delta_\theta = O(1/T)$ could be achieved for an arbitrary desired standard deviation, where $T = \sum \tau$ is the total duration of the estimation process.

In the next subsection, we discuss the problems of DQC1 model when it is directly applied to estimate the hyperfine interaction in the NV center. Before that, we mention a useful extension (which can be readily verified) of this model: the analytical expressions for the quantity estimated by the measurement [e.g., $\langle \hat{X} \rangle = \cos(\theta\tau)$ for the DQC1 model and $\langle \hat{Z} \rangle = \cos(A\tau)$ for our protocol, see Eq. (5)] remains valid for a more general initial state $\rho_{\text{tar}} = 1/2 + q_z \sigma_z/2$ of the target qubit with an arbitrary polarization q_z . This fact is especially important for estimating the hyperfine interaction in the NV center since in this case, initializing the control qubit (the electron spin in the NV center) will partially polarize the target qubit (the ¹⁵N nuclear spin in the NV center).¹⁶

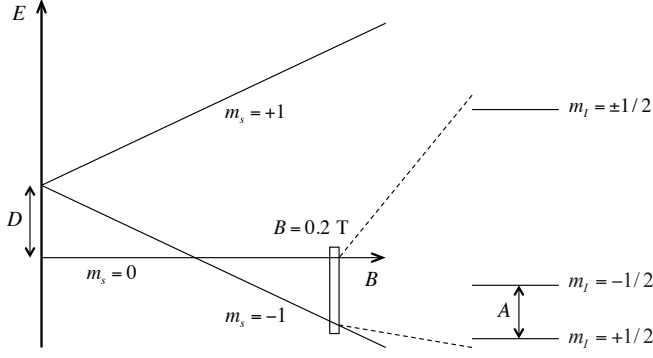


FIG. 2. Energy level diagram of the ground state of an NV center in diamond. The hyperfine energy splitting at $B = 0.2$ T is sketched within the $|m_s = 0\rangle$ and $|m_s = -1\rangle$ manifold. $D = 2.87$ GHz is the zero field splitting of the electron spin, and A is the longitudinal hyperfine interaction to be estimated. The nuclear Zeeman splitting is omitted in the diagram.

B. Direct application of DQC1 parameter estimation to NV center

We consider a negatively charged NV center in diamond consisting of a substitutional ^{15}N atom and a neighboring carbon vacancy. Its electronic ground state is a two-electron spin triplet described by a spin-1 operator $\hat{\mathbf{S}}$, with a zero-field splitting $D \approx 2.87$ GHz (described by the term $D\hat{S}_z^2$) between the $|m_s = 0\rangle$ state and the $|m_s = \pm 1\rangle$ states. Under an external magnetic field B along the N-V axis (defined as the z direction), the Zeeman term $g_e\mu_B B\hat{S}_z$ with $g_e = 2.0023$ shifts the state $|m_s = +1\rangle$ away from the other two states under a moderate magnetic field $B \sim 0.2$ T (see Fig. 2). Thus we identify $|0\rangle \equiv |m_s = 0\rangle$ and $|1\rangle \equiv |m_s = -1\rangle$ as the two states of the control qubit of the DQC1 model and use $\hat{X}, \hat{Y}, \hat{Z}$ as the three Pauli matrices for this qubit. The electron spin $\hat{\mathbf{S}}$ is coupled to the neighboring ^{15}N nuclear spin-1/2 $\hat{\mathbf{I}}$ (with the two-fold degeneracy lifted by the Zeeman term $g_N\mu_N B\hat{I}_z$, where $g_N = -0.5664$ ¹⁷) through the hyperfine interaction $A\hat{S}_z\hat{I}_z + (A_\perp/2)(\hat{S}_+\hat{I}_- + \hat{S}_-\hat{I}_+)$, where $A \approx 3.03$ MHz and $A_\perp \approx 3.65$ MHz.¹⁷ We regard this nuclear spin-1/2 as the mixed-state target qubit of the DQC1 model and use $\hat{\sigma}_x, \hat{\sigma}_y, \hat{\sigma}_z$ as the three Pauli matrices $2\hat{I}_x, 2\hat{I}_y, 2\hat{I}_z$ for this qubit. The diagonal part $A\hat{S}_z\hat{I}_z$ of the hyperfine interaction makes the nuclear (electron) spin splitting energy dependent on the state of the electron (the nucleus). Thus $A\hat{S}_z\hat{I}_z$ plays the central role in coherent control and readout of the electron and nuclear spin states. The hyperfine interaction strength A is the parameter to be estimated.

In the two-qubit subspace, the Hamiltonian $\hat{H} = \hat{H}_0 + \hat{H}_{\text{mix}}$ consists of the diagonal part

$$\hat{H}_0 = \frac{1}{2}g_N\mu_N B\hat{\sigma}_z + |1\rangle\langle 1| \otimes (D' - \frac{1}{2}A\hat{\sigma}_z)$$

and the off-diagonal part

$$\hat{H}_{\text{mix}} = (A_\perp/\sqrt{2})(|0, \downarrow\rangle\langle 1, \uparrow| + |1, \uparrow\rangle\langle 0, \downarrow|).$$

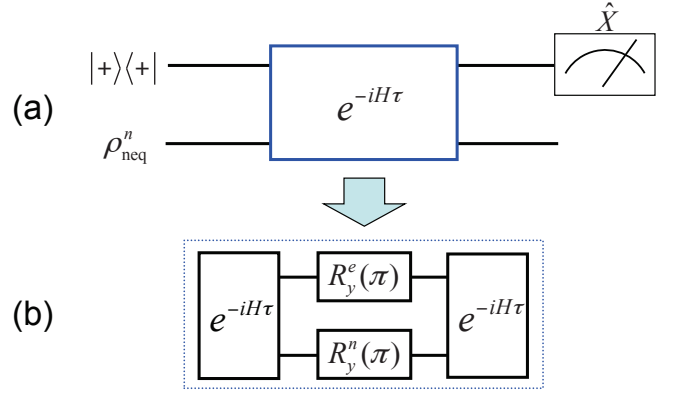


FIG. 3. (a) Direct application of the DQC1 model to estimate the hyperfine interaction strength A in NV center. (b) Combination of spin echo and the DQC1 model.

The diagonal part \hat{H}_0 accounts for the free nuclear spin precession with angular frequency $g_N\mu_N B$, the free electron spin precession with angular frequency $D' \equiv D - g_e\mu_B B$, and the projection $|1\rangle\langle 1| \otimes (-A\hat{\sigma}_z/2)$ of the diagonal hyperfine interaction $A\hat{S}_z\hat{I}_z$ in the two-qubit subspace. The off-diagonal part \hat{H}_{mix} is the projection of the off-diagonal hyperfine interaction $(A_\perp/2)(\hat{S}_+\hat{I}_- + \hat{S}_-\hat{I}_+)$ in the two-qubit subspace. The diagonal hyperfine interaction term $|1\rangle\langle 1| \otimes (-A\hat{\sigma}_z/2)$ in \hat{H}_0 corresponds to \hat{H}_{DQC1} in Eq. (1) with $\theta \leftrightarrow (-A/2)$. It makes the precession frequency ω_e of the electron spin dependent on the hyperfine interaction strength A and the nuclear spin state: $\omega_{e,\uparrow} = D' - A/2$ for the nuclear spin state being $|\uparrow\rangle$ and $\omega_{e,\downarrow} = D' + A/2$ for the nuclear spin state being $|\downarrow\rangle$. Therefore, following the procedure in Fig. 1, the interaction strength A is encoded as a phase of the electron spin and subsequently extracted by estimating $\langle \hat{X} \rangle$.

As schematically shown in Fig. 3(a), the electron spin needs to be prepared in the superposition $(|0\rangle + |1\rangle)/\sqrt{2}$. This can be achieved by optical pumping¹⁸ followed by a coherent rotation. However, this preparation process inevitably influences the nuclear spin and changes its state from the unpolarized thermal equilibrium state $\hat{\rho}_{\text{eq}}^n = \hat{I}/2$ to a state $\hat{\rho}_{\text{eq}}^n = \hat{I}/2 + q_z\hat{\sigma}_z/2$ with a finite polarization $q_z = \text{Tr}[\hat{\rho}_{\text{eq}}^n\hat{\sigma}_z]$.¹⁶ Then the two qubits evolve under the Hamiltonian \hat{H} for a duration τ , followed by a measurement of $\langle \hat{X} \rangle$. Below we calculate $\langle \hat{X} \rangle$ without \hat{H}_{mix} and then taking it into account by perturbation theory.

Without \hat{H}_{mix} , the two qubits are driven by \hat{H}_0 , which has four eigenstates $|0, \uparrow\rangle, |0, \downarrow\rangle, |1, \uparrow\rangle, |1, \downarrow\rangle$. The physics is similar to the DQC1 model described in the previous subsection:

- If the nuclear spin is in the spin-up state $|\uparrow\rangle$, then \hat{H}_0 drives the precession of the electron spin qubit with angular frequency $\omega_{e,\uparrow}$ and the repeated measurements of \hat{X} estimate $\langle \hat{X} \rangle_\uparrow = \cos(\omega_{e,\uparrow}\tau)$.
- If the nuclear spin is in the spin-down state $|\downarrow\rangle$, then \hat{H}_0 drives the precession of the electron spin qubit with angular frequency $\omega_{e,\downarrow}$ and the repeated measurements of \hat{X} estimate $\langle \hat{X} \rangle_\downarrow = \cos(\omega_{e,\downarrow}\tau)$.

- Now the nuclear spin is in an incoherent mixture of $|\uparrow\rangle$ [with weight $(1+q_z)/2$] and $|\downarrow\rangle$ [with weight $(1-q_z)/2$]. Then the repeated measurements of \hat{X} estimate the weighted average of $\langle\hat{X}\rangle_\uparrow$ and $\langle\hat{X}\rangle_\downarrow$:

$$\langle\hat{X}\rangle = \frac{1+q_z}{2}\langle\hat{X}\rangle_\uparrow + \frac{1-q_z}{2}\langle\hat{X}\rangle_\downarrow. \quad (3)$$

Then we consider the complications caused by the off-diagonal part \hat{H}_{mix} . To reduce its detrimental effect on the parameter estimation, we consider a suitable magnetic field strength (e.g., $B = 0.2$ T, as indicated in Fig. 2 and used in our estimation, see Sec. IV C) so that $|D'| \gg |A_\perp|$. In this case, we can use perturbation theory to treat \hat{H}_{mix} , which modifies the eigenstates and eigenenergies of the two-qubit Hamiltonian $\hat{H} = \hat{H}_0 + \hat{H}_{\text{mix}}$:

1. \hat{H}_{mix} changes the eigenstates of \hat{H} from $[|0, \uparrow\rangle, |0, \downarrow\rangle, |1, \uparrow\rangle, |1, \downarrow\rangle]$ to $[|0, \uparrow\rangle, |\widetilde{0}, \downarrow\rangle, |\widetilde{1}, \uparrow\rangle, |1, \downarrow\rangle]$, where

$$\begin{aligned} |\widetilde{0}, \downarrow\rangle &= [1 - O(\eta^2)]|0, \downarrow\rangle + O(\eta)|1, \uparrow\rangle, \\ |\widetilde{1}, \uparrow\rangle &= [1 - O(\eta^2)]|1, \uparrow\rangle + O(\eta)|0, \downarrow\rangle, \end{aligned}$$

and $\eta \equiv A_\perp/(D' + g_N\mu_N B - A/2) \sim 10^{-3}$ for $B = 0.2$ T. In other words, \hat{H}_{mix} introduces new $O(\eta)$ components into the eigenstates. It can be readily verified that this changes $\langle\hat{X}\rangle$ by $O(\eta^2)$.

2. \hat{H}_{mix} changes the eigenenergy of $|0, \downarrow\rangle$ ($|1, \uparrow\rangle$) by a small amount $-\delta$ ($+\delta$), where $\delta = \eta A_\perp/2 + O(\eta^2 A_\perp)$. This in turn changes the precession frequencies of the electron spin from $\omega_{e,\mu}$ to $\tilde{\omega}_{e,\mu} = \omega_{e,\mu} + \delta$ ($\mu = \uparrow, \downarrow$). Therefore, the average value $\langle\hat{X}\rangle$ is obtained from Eq. (3) by renormalizing $\omega_{e,\mu}$ with $\tilde{\omega}_{e,\mu}$ ($\mu = \uparrow, \downarrow$).

Collecting both corrections discussed above, we obtain

$$\begin{aligned} \langle\hat{X}\rangle &= \cos[(D' + \delta)\tau] \cos\left(\frac{A}{2}\tau\right) \\ &+ q_z \sin[(D' + \delta)\tau] \sin\left(\frac{A}{2}\tau\right) + O(\eta^2). \end{aligned} \quad (4)$$

It contains not only A but also undesired parameters such as D' (free electron spin precession frequency), δ (energy shift by \hat{H}_{mix}), and q_z (partial nuclear spin polarization). For an accurate estimation of A , it is desirable to eliminate these undesired parameters from $\langle\hat{X}\rangle$ by modifying the DQC1 protocol.

III. ELIMINATING UNDESIED PARAMETERS BY SPIN ECHO

To remove the dependence on the undesired parameters in $\langle\hat{X}\rangle$, we combine the DQC1 model with the spin-echo technique by replacing the free evolution $e^{-i\hat{H}\tau}$ with the composite evolution [see Fig. 3(b)]

$$\hat{U}_{\text{com}} = e^{-i\hat{H}\tau} \hat{R}_y^n(\pi) \hat{R}_y^n(\pi) e^{-i\hat{H}\tau} = \hat{R}_y^n(\pi) \hat{R}_y^n(\pi) \left(e^{-i(\hat{\sigma}_y \hat{Y} \hat{H} \hat{Y} \hat{\sigma}_y)\tau} e^{-i\hat{H}\tau} \right),$$

which consists of an electron spin π rotation $\hat{R}_y^e(\pi) = e^{-i\pi\hat{Y}/2} = -i\hat{Y}$ and a nuclear spin π rotation $\hat{R}_y^n(\pi) = e^{-i\pi\hat{\sigma}_y/2} = -i\hat{\sigma}_y$ sandwiched by the free evolution $e^{-i\hat{H}\tau}$. This composite evolution contains a spin echo (the part inside the parenthesis) for the electron and the nucleus, which eliminates the free precession of the electron spin and the nuclear spin. To analyze \hat{U}_{com} in more detail, we first ignore the off-diagonal part \hat{H}_{mix} and then take it into account by perturbation theory.

Without \hat{H}_{mix} , the Hamiltonian $\hat{H}' \equiv \hat{\sigma}_y \hat{Y} \hat{H} \hat{Y} \hat{\sigma}_y$ commutes with \hat{H} . Thus \hat{U}_{com} reduces to

$$\hat{U}_{\text{com}}^{(0)} = \hat{R}_y^e(\pi) \hat{R}_y^n(\pi) e^{-i(\hat{H}' + \hat{H})\tau} = \hat{R}_y^e(\pi) \hat{R}_y^n(\pi) e^{-iA\tau\hat{\sigma}_z/2} e^{-i\hat{H}_{\text{echo}}\tau},$$

where $\hat{H}_{\text{echo}} = |1\rangle\langle 1| \otimes (-A\hat{\sigma}_z)$ corresponds to \hat{H}_{DQC1} in Eq. (1) with $\theta \leftrightarrow -A$. The operation $\hat{R}_y^n(\pi) e^{-iA\tau\hat{\sigma}_z/2}$ on the nuclear spin alone can be dropped since it does not influence our measurement on the electron spin. Therefore, the composite evolution becomes $\hat{U}_{\text{com}}^{(0)} = \hat{R}_y^e(\pi) e^{-i\hat{H}_{\text{echo}}\tau}$, in which all the undesired parameters have been eliminated.

In the presence of \hat{H}_{mix} , \hat{H}' consists of the diagonal part

$$\hat{H}'_0 = -\frac{1}{2}g_N\mu_N B\hat{\sigma}_z + \frac{1}{2}A\hat{\sigma}_z - |1\rangle\langle 1| \otimes (D' + \frac{1}{2}A\hat{\sigma}_z)$$

and the off-diagonal part \hat{H}_{mix} . Similar to the two-step analysis leading to Eq. (4), \hat{H}_{mix} modifies the eigenstates and eigenenergies of $\hat{H} = \hat{H}_0 + \hat{H}_{\text{mix}}$ and $\hat{H}' = \hat{H}'_0 + \hat{H}_{\text{mix}}$:

1. \hat{H}_{mix} introduces new $O(\eta)$ components into the eigenstates of \hat{H} and \hat{H}' . This changes $\langle\hat{X}\rangle$ by $O(\eta^2)$.
2. For the Hamiltonian \hat{H} , the presence of \hat{H}_{mix} changes the eigenenergy of $|0, \downarrow\rangle$ ($|1, \uparrow\rangle$) by $-\delta$ ($+\delta$). For the Hamiltonian \hat{H}' , the presence of \hat{H}_{mix} changes the eigenenergy of $|0, \downarrow\rangle$ ($|1, \uparrow\rangle$) by $+\delta$ ($-\delta$). In other words, the opposite energy shifts for \hat{H} and \hat{H}' induced by \hat{H}_{mix} cancel each other in the evolution \hat{U}_{com} .

For $\langle\hat{X}\rangle$, the composite evolution including both corrections discussed above is equivalent to

$$\hat{U}_{\text{com}} = \hat{R}_y^e(\pi) e^{-i\hat{H}_{\text{echo}}\tau} + O(\eta^2),$$

i.e., the spin echo eliminates all the named undesired parameters and the effective evolution \hat{U}_{com} for the NV center recovers the DQC1 evolution $e^{-i\hat{H}_{\text{DQC1}}\tau}$ up to a trivial electron spin π rotation $\hat{R}_y^e(\pi)$.

IV. QUANTUM MEASUREMENT PROTOCOL OF HYPERFINE INTERACTION

In this section, first we give the quantum circuit for a single estimation of the hyperfine interaction strength A in the NV center. Second, we describe in detail the procedure of the entire estimation protocol: the successive adaptation of the quantum circuit for dramatically reduced standard deviation by combining our prior knowledge with the outcomes of the previous measurements through adaptive Bayesian inference.

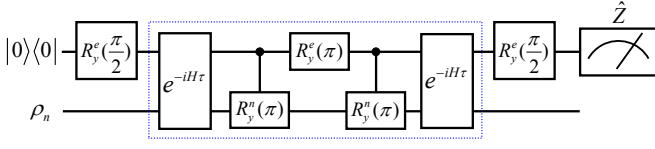


FIG. 4. Quantum circuit for a single estimation of the hyperfine interaction strength A in the NV center.

Third, we demonstrate that this protocol approaches the QML $\Delta_{\text{QML}} = O(1/T)$ for the ideal case. Finally, we include the essential errors (the nuclear spin rotation error and the electron spin decoherence) and show that our protocol still exceeds the SQL.

A. Quantum estimation circuit

Fig. 4 gives the sequence of quantum operations for a single estimation of the hyperfine interaction strength A in the NV center:

1. The electron spin is prepared into the pure state $|0\rangle$ by optical pumping.¹⁸ A subsequent $\pi/2$ rotation $\hat{R}_y^e(\pi/2)$ initializes the electron spin into the superposition $|+\rangle = (|0\rangle + |1\rangle)/\sqrt{2}$. The nuclear spin is a partially polarized state $\hat{\rho}_n = \hat{I}/2 + q_z \hat{\sigma}_z/2$. This initial density matrix $\hat{\rho}_{\text{initial}} = |+\rangle\langle+| \otimes \hat{\rho}_n$ coincides with the initial density matrix $\hat{\rho}_{\text{DQC1}} = |+\rangle\langle+| \otimes \hat{\rho}_{\text{tar}}$ of the DQC1 model, where the target qubit state $\hat{\rho}_{\text{tar}}$ also has an arbitrary polarization, as discussed at the end of Sec. II A.
2. The two qubits experience a composite evolution (within the dashed box in Fig. 4), which consists of a free evolution $e^{-iH\tau}$, a controlled nuclear spin π rotation $\tilde{R}_y^n(\pi) = |1\rangle\langle 1| \otimes (-i\hat{\sigma}_y) + |0\rangle\langle 0|$, an electron spin rotation $\hat{R}_y^e(\pi)$, another controlled nuclear spin π rotation $\tilde{R}_y^n(\pi)$, and another free evolution $e^{-iH\tau}$. The equality $\tilde{R}_y^n(\pi)\hat{R}_y^e(\pi)\tilde{R}_y^n(\pi) = \hat{R}_y^n(\pi)\hat{R}_y^e(\pi)$ shows that this composite evolution coincides with \hat{U}_{com} in Sec. III.
3. A $\pi/2$ rotation $\hat{R}_y^e(\pi/2)$ is applied to the electron spin, followed by a measurement of \hat{Z} through optical methods.^{4,19} This measurement estimates

$$\begin{aligned} \langle \hat{Z} \rangle &= \text{Tr} \hat{Z} \hat{R}_y^e(\pi/2) \hat{U}_{\text{com}} \hat{\rho}_{\text{initial}} \hat{U}_{\text{com}}^\dagger [\hat{R}_y^e(\pi/2)]^\dagger \\ &= \text{Tr} \hat{X} e^{-i\hat{H}_{\text{echo}}\tau} \hat{\rho}_{\text{initial}} e^{i\hat{H}_{\text{echo}}\tau} + O(\eta^2). \end{aligned}$$

Since the evolution $e^{-i\hat{H}_{\text{echo}}\tau} = e^{-i\hat{H}_{\text{DQC1}}\tau}|_{\theta \rightarrow -A}$ has the same form as the DQC1 model, the average value is

$$\langle \hat{Z} \rangle = \cos(A\tau) + O(\eta^2). \quad (5)$$

The electron spin rotation $\hat{R}_y^e(\pi/2)$ [$\hat{R}_y^e(\pi)$] in the circuit is achieved by a $\pi/2$ pulse (π pulse) with the central frequency $|D'|$ and the bandwidth $\gg A/2$, so that both transitions $|0, \uparrow\rangle \leftrightarrow |1, \uparrow\rangle$ and $|0, \downarrow\rangle \leftrightarrow |1, \downarrow\rangle$ are equally excited. The

controlled nuclear spin rotation $\tilde{R}_y^n(\pi)$ is achieved by a π pulse centered at the resonant frequency $A - g_N \mu_N B - \delta$ of the transition $|1, \uparrow\rangle \rightarrow |1, \downarrow\rangle$. The duration τ of the free evolution can be chosen in the experiment as $\tau > 1/A \sim 0.1 \mu\text{s}$. The electron spin rotation occurs within a few nanoseconds and hence can be regarded as instantaneous.^{20,21} However, the controlled nuclear spin π rotation takes $\tau_n \sim$ a few microseconds, comparable to the free evolution time τ . Detailed analysis in appendix A shows that incorporation of τ_n amounts to replacing the free evolution time τ in Eq. (5) by the sum $(\tau + \tau_n)$. For brevity, we use τ to denote $(\tau + \tau_n)$ from now on.

In arriving at Eq. (5), we have assumed that all the gate operations in the circuit and the measurements of \hat{Z} are free of errors. In a realistic experiment, the most basic errors include the deviation of the nuclear spin rotation angle from π in the controlled π rotation $\tilde{R}_y^n(\pi)$ and the finite electron spin coherence time T_2^e :

- Nuclear spin rotation error. The two controlled nuclear spin π rotations $\tilde{R}_y^n(\pi)$ in the quantum estimation circuit (Fig. 4) are subjected to random errors, which may come from our limited prior knowledge (which becomes more and more precise after each successive estimation step) about the interaction strength A or other experimental sources. For the actual rotation angle $(\pi + 2\epsilon)$ differing from π by an error 2ϵ , the actual controlled rotation $\tilde{R}_y^n(\pi, \epsilon) = \tilde{R}_y^n(\pi) + \delta_y^n(\pi)$ differs from the ideal one $\tilde{R}_y^n(\pi)$ by

$$\delta_y^n(\pi) = |1\rangle\langle 1| \otimes (-\epsilon + i\frac{\epsilon^2}{2}\hat{\sigma}_y) + O(\epsilon^3).$$

For the first controlled rotation being $\tilde{R}_y^n(\pi, \epsilon_a)$ and the second controlled rotation being $\tilde{R}_y^n(\pi, \epsilon_b)$, the actual quantity estimated by the quantum circuit $M(\tau)$ is

$$\begin{aligned} \langle \hat{Z}_\epsilon \rangle &= \left(1 - \frac{\langle \epsilon_a^2 \rangle + \langle \epsilon_b^2 \rangle}{2} \right) \cos(A\tau) \\ &\quad + \langle \epsilon_a \epsilon_b \rangle + \langle \epsilon_a \rangle O(\eta) + \langle \epsilon_b \rangle O(\eta) + O(\eta^2), \end{aligned}$$

The first source of error is our ignorance about A . In the k -th estimation step, our limited prior knowledge about A (as quantified by the standard deviation Δ_{k-1} , see Sec. IV B) and hence the resonant frequency $A - g_N \mu_N B - \delta$ of the transition $|1, \uparrow\rangle \rightarrow |1, \downarrow\rangle$ makes it impossible to construct an exact π pulse for this transition. The typical detuning for this transition is Δ_{k-1} . The typical rotation angle deviates from the ideal value π by an amount $\pi \Delta_{k-1}^2 / (2\Omega^2) \sim 10^{-3}$, the same order of magnitude as $O(\eta)$, for the Rabi frequency $\Omega = 500 \text{ kHz}$ used in our estimation. Thus every term in the second line of the above equation has the same order of $\sim 10^{-6}$, which allows us to replace the second line by $O(\eta^2)$. For ϵ_a and ϵ_b being independent, we obtain

$$\langle \hat{Z}_\epsilon \rangle = (1 - \epsilon^2) \cos(A\tau) + O(\eta^2),$$

where $\epsilon^2 = \langle \epsilon_a^2 \rangle = \langle \epsilon_b^2 \rangle$. For other experimental sources, the errors are typically random with $\langle \epsilon_a \rangle = \langle \epsilon_b \rangle = \langle \epsilon_a \epsilon_b \rangle = 0$, so that the above equation still holds.

- Electron spin decoherence. The electron spin in the NV center is subjected to decoherence by the surrounding ^{13}C nuclear spin bath. The coherence time of the electron spin in the ground state is $T_2^e \sim 350 \mu\text{s}$ under the natural abundance of the ^{12}C isotope (98.8%), and it is extended to 1.8 ms under the ultrapure ^{12}C abundance (99.7%) at room temperature.^{1,22} By incorporating the electron spin relaxation (with the relaxation time²³ $T_1^e = 5.9 \text{ ms}$) and decoherence in the Lindblad form, it is straightforward to show that the quantity estimated by the quantum circuit is no longer Eq. (5) but instead

$$\langle \hat{Z}_d \rangle = e^{-2\tau/T_2^e} \cos(A\tau) + O(\eta^2).$$

In summary, in the presence of errors, the quantity estimated by the quantum circuit in Fig. 4 is given by

$$\langle \hat{Z} \rangle = Q(\tau) \cos(A\tau) + O(\eta^2), \quad (6)$$

where $Q(\tau) = 1 - \varepsilon^2$ for the nuclear spin rotation error of magnitude ε and $Q(\tau) = e^{-2\tau/T_2^e}$ for a finite electron spin coherence time T_2^e . In our estimation, we use $B = 0.2 \text{ T}$ so that the correction for the hyperfine interaction $O(\eta^2) \sim 10^{-6}$.

B. Estimation procedure

We use $M(\tau)$ to denote the quantum estimation circuit in Fig. 4, whose total duration is 2τ . A single run of the circuit $M(\tau)$ returns two outcomes: $+1$ for the electron spin in the state $|0\rangle$ or -1 for the electron spin in the state $|1\rangle$, with corresponding probabilities $p_{\pm 1} = [1 \pm \langle \hat{Z} \rangle]/2$. An estimator of the average value $\langle \hat{Z} \rangle$ [Eq. (6)] is obtained by averaging over the outcomes of repeated running of the circuit. For example, averaging over N measurements produces Z , a single estimator of $\langle \hat{Z} \rangle$. By the central limit theorem, for relatively large N (e.g., $N \gtrsim 100$), *this estimator obeys the Gaussian distribution $N(\langle \hat{Z} \rangle, \zeta)$ centered at $\langle \hat{Z} \rangle$ with a standard deviation $\zeta = 1/\sqrt{N}$.* Alternatively, we can also say that *the average value $\langle \hat{Z} \rangle$ obeys the Gaussian distribution $N(Z, \zeta)$* , which actually means that the difference $\langle \hat{Z} \rangle - Z$ obeys the Gaussian distribution $N(0, \zeta)$.

The estimation begins with a prior knowledge of the hyperfine interaction strength A . It is quantified by a Gaussian distribution $N(A_0, \Delta_0)$ centered at A_0 with a relatively large standard deviation Δ_0 , which quantifies our ignorance about A . This prior knowledge tells us, with a 95% confidence, that A lies within the interval $[A_0 - 1.96\Delta_0, A_0 + 1.96\Delta_0]$. From the prior knowledge $N(A_0, \Delta_0)$, we construct the quantum circuit $M(\tau_1)$ for the first estimation, which provides a new knowledge about A , as quantified by a Gaussian distribution $N(\bar{A}_1, \bar{\Delta}_1)$. Through the Bayesian inference, this new knowledge is combined with the prior knowledge to produce an updated knowledge about A , quantified by a Gaussian distribution $N(A_1, \Delta_1)$ with a smaller standard deviation $\Delta_1 < \Delta_0$. Therefore, the first estimation step refines our knowledge about A from $N(A_0, \Delta_0)$ to $N(A_1, \Delta_1)$ (with $\Delta_1 < \Delta_0$), which in turn serves as the prior knowledge of the next estimation

step. By iterating this procedure, the standard deviation of the Gaussian distribution quantifying our ignorance about A would decrease successively as $\Delta_0 > \Delta_1 > \Delta_2 > \dots$. The iteration is stopped at the K -th step when the desired standard deviation Δ_{desire} is achieved: $\Delta_K \leq \Delta_{\text{desire}}$. Below, we describe the above estimation procedures in more detail.

1. Gaining knowledge about A from measurements

In the k -th estimation step ($k = 1, 2, \dots$), the prior knowledge about the hyperfine interaction strength A is quantified by the Gaussian distribution $N(A_{k-1}, \Delta_{k-1})$. Suppose that τ_k has been properly chosen (to be discussed shortly). By running the circuit $M(\tau_k)$ for a relatively large number $N_k (\gtrsim 100)$ of times, we obtain an estimator Z_k of $\langle \hat{Z} \rangle_k \equiv Q(\tau_k) \cos(A\tau_k) + O(\eta^2)$ with a standard deviation $\zeta_k = 1/\sqrt{N_k}$. This knowledge tells us that $\langle \hat{Z} \rangle_k$ obeys the Gaussian distribution $N(Z_k, \zeta_k)$. We need to convert this distribution of $\langle \hat{Z} \rangle_k$ to a distribution of A . For a general τ_k , the relation between $\langle \hat{Z} \rangle_k$ and A is nonlinear and the conversion from $\langle \hat{Z} \rangle_k$ to A results in a non-Gaussian distribution of A , with a characteristic width

$$\frac{\zeta_k}{|\partial \langle \hat{Z} \rangle_k / \partial A|} = \frac{\zeta_k}{Q(\tau_k) \tau_k |\sin(A\tau_k)|}.$$

Now we determine τ_k according to two requirements:

1. The distribution of A should be Gaussian (i.e., the relation between $\langle \hat{Z} \rangle_k$ and A should be linear), so that analytical results can be obtained. Based on our prior knowledge $N(A_{k-1}, \Delta_{k-1})$ about A , the conditions $A_{k-1}\tau_k = \pi/2 + 2\pi \times \text{integer}$ and $\Delta_{k-1}\tau_k \ll 1$ enable the Taylor expansion $\langle \hat{Z} \rangle_k = (A_{k-1} - A)Q(\tau_k)\tau_k + \delta_k + O(\eta^2)$ with $\delta_k \approx Q(\tau_k)(\Delta_{k-1}\tau_k)^3/6$. For $\delta_k, O(\eta^2) \ll \zeta_k, |\langle \hat{Z} \rangle_k|$, the correction terms $\delta_k + O(\eta^2)$ can be safely dropped, so that the relation between $\langle \hat{Z} \rangle_k$ and A becomes linear and the distribution of A becomes Gaussian $N(\bar{A}_k, \bar{\Delta}_k)$ with

$$\bar{A}_k = A_{k-1} - \frac{Z_k}{Q(\tau_k)\tau_k}, \quad (7a)$$

$$\bar{\Delta}_k = \frac{\zeta_k}{Q(\tau_k)\tau_k} = \frac{1}{Q(\tau_k)\tau_k \sqrt{N_k}}. \quad (7b)$$

The distribution $N(\bar{A}_k, \bar{\Delta}_k)$ of A tells us, with a 95% confidence, that A lies in the interval $[\bar{A}_k - 1.96\bar{\Delta}_k, \bar{A}_k + 1.96\bar{\Delta}_k]$.

2. For maximal precision of the estimation, the standard deviation $\bar{\Delta}_k$ should be minimized, i.e., $Q(\tau_k)\tau_k$ should be maximized.

Eq. (7b) shows that the standard deviation $\bar{\Delta}_k$ of the measurement of A is equal to the standard deviation $\zeta_k = 1/\sqrt{N_k}$ of the measurement of $\langle \hat{Z} \rangle_k$ divided by $Q(\tau_k)\tau_k$:

- For $Q(\tau_k) = 1$ (i.e., no errors), the standard deviation $\bar{\Delta}_k$ is reduced upon the increase of τ_k , which can be interpreted as a repetition of the circuit operations (as

enclosed in the dashed box in Fig. 4) before the measurement is made. This is equivalent to a multiround protocol suggested by Giovannetti *et al.*⁷. Therefore, the dependence $\bar{\Delta}_k \propto 1/\tau_k$ implies the QML.

- The standard deviation $\bar{\Delta}_k$ is reduced upon the increase of N_k . The dependence $\bar{\Delta}_k \propto 1/\sqrt{N_k}$ implies the SQL.

In summary, for optimal performance, we should first choose ζ_k (or equivalently N_k) subjected to the constraint

$$O(\eta^2) \ll \zeta_k \ll 1 \quad (8)$$

and then choose τ_k to maximize $Q(\tau_k)\tau_k$, subjected to the constraints

$$A_{k-1}\tau_k = \frac{\pi}{2} + 2m_k\pi, \quad (9a)$$

$$\frac{(\Delta_{k-1}\tau_k)^3}{6} \ll \zeta_k, \quad (9b)$$

$$Q(\tau_k)\Delta_{k-1}\tau_k \gg O(\eta^2), \quad (9c)$$

where $m_k \in \mathbb{Z}$ and $O(\eta^2) \sim 10^{-6}$ for $B = 0.2$ T. The constraint $\zeta_k \ll 1$ ensures the validity of our Gaussian distribution assumption for $\langle \hat{Z} \rangle_k$, while other constraints ensure the validity of the formula $\langle \hat{Z} \rangle_k \approx (A_{k-1} - A)Q(\tau_k)\tau_k$. The error of the linear expansion can be dropped if $\delta_k \ll \zeta_k$, which gives Eq. (9b) with $Q(\tau_k) \leq 1$. Eq. (9c) denotes the condition to drop $O(\eta^2)$ in $\langle \hat{Z} \rangle_k$. Note that the constraints [Eqs. (9)] on τ_k have no solution under certain conditions, e.g., when $Q(\tau_k) \lesssim O(\eta^2)/(\zeta_k)^{1/3}$. Therefore, for more flexible choice of τ_k , the standard deviation ζ_k of the measurement of $\langle \hat{Z} \rangle_k$ should not be too small.

2. Combining new knowledge with prior knowledge

In the previous subsection, we have spent N_k runs of the circuit $M(\tau_k)$ to obtain the new knowledge $\mathcal{N}(\bar{A}_k, \bar{\Delta}_k)$ about A . To make use of the resources spent in obtaining the prior knowledge $\mathcal{N}(A_{k-1}, \Delta_{k-1})$, we use the Bayesian inference, which combines our new knowledge $\mathcal{N}(\bar{A}_k, \bar{\Delta}_k)$ with the prior knowledge $\mathcal{N}(A_{k-1}, \Delta_{k-1})$. It gives an updated Gaussian distribution $\mathcal{N}(A_k, \Delta_k)$ centered at

$$A_k = \frac{A_{k-1}/\Delta_{k-1}^2 + \bar{A}_k/\bar{\Delta}_k^2}{1/\Delta_{k-1}^2 + 1/\bar{\Delta}_k^2} \quad (10a)$$

(which is a weighted average of A_{k-1} with weight $1/\Delta_{k-1}^2$ and \bar{A}_k with weight $1/\bar{\Delta}_k^2$) with a standard deviation Δ_k determined by

$$\frac{1}{\Delta_k^2} = \frac{1}{\Delta_{k-1}^2} + \frac{1}{\bar{\Delta}_k^2}. \quad (10b)$$

This updated knowledge $\mathcal{N}(A_k, \Delta_k)$ tells us, with a 95% confidence, that A lies in the refined interval $[A_k - 1.96\Delta_k, A_k + 1.96\Delta_k]$. The inequalities $\Delta_k < \Delta_{k-1}$ and $\Delta_k < \bar{\Delta}_k$ reveal that the combination of $\mathcal{N}(A_{k-1}, \Delta_{k-1})$ and $\mathcal{N}(\bar{A}_k, \bar{\Delta}_k)$ gives us a more precise knowledge about A .

For very accurate measurement compared with the prior knowledge, i.e., $\bar{\Delta}_k \ll \Delta_{k-1}$, Eqs. (10a) and (10b) reduce to $A_k \approx \bar{A}_k$ and $\Delta_k \approx \bar{\Delta}_k$, suggesting that the updated knowledge is dominated by the measurement. By contrast, for inaccurate measurement $\bar{\Delta}_k \gg \Delta_{k-1}$, the updated knowledge $A_k \approx A_{k-1}$ and $\Delta_k \approx \Delta_{k-1}$ is dominated by the prior knowledge.

C. Ideal case: approaching quantum metrology limit

In this subsection, we demonstrate the QML scaling of our estimation protocol in the ideal case, i.e., in the absence of any errors (e.g., operation errors, relaxation, and decoherence). For simplicity, we assume that in each estimation step, we run the quantum circuit for the same number of times $N_1 = N_2 = \dots \equiv N$, corresponding to $\zeta_1 = \zeta_2 = \dots \equiv \zeta \equiv 1/\sqrt{N}$.

Up to the K -th estimation step, the total duration of the our estimation process (identified as the total amount of resources spent) is

$$R_K = N \sum_{k=1}^K 2\tau_k \equiv N\tau_K^{\text{tot}}.$$

To see the scaling of the precision $1/\Delta_K^2$ with respect to R_K , we take the first estimation step as a reference. Further, we take $\Delta_0 = \infty$ to exclude the contribution from the prior knowledge $\mathcal{N}(A_0, \Delta_0)$, so that all our knowledge about A comes from the resources R_K spent in our protocol. Then, the QML limit $\Delta_{K,\text{QML}}$ is defined by $\Delta_{K,\text{QML}}/\Delta_1 \equiv 1/(R_K/R_1)$, while the SQL limit $\Delta_{K,\text{SQL}}$ is defined by $\Delta_{K,\text{SQL}}/\Delta_1 \equiv 1/\sqrt{R_K/R_1}$. Using $R_1 = 2N\tau_1$ and $\Delta_1 = 1/(\tau_1\sqrt{N})$, we obtain

$$\frac{1}{\Delta_{K,\text{QML}}^2} = N \left(\sum_{k=1}^K \tau_k \right)^2, \quad (11)$$

$$\frac{1}{\Delta_{K,\text{SQL}}^2} = N\tau_1 \sum_{k=1}^K \tau_k, \quad (12)$$

$$\frac{1}{\Delta_K^2} = N \sum_{k=1}^K \tau_k^2.$$

First, we compare Δ_K with the QML limit $\Delta_{K,\text{QML}}$ and the SQL limit $\Delta_{K,\text{SQL}}$ and discuss the condition for approaching the QML:

1. The inequality $\Delta_K > \Delta_{K,\text{QML}}$ can be readily verified. This manifests the QML precision $1/\Delta_{K,\text{QML}}^2$ as the upper precision bound. To achieve the QML, $\{\tau_k\}$ should satisfy $\tau_K \gg \tau_{K-1} \gg \dots \gg \tau_1$, so that the total amount of resources is dominated by the final estimation step and hence $\Delta_K \approx \Delta_{K,\text{QML}} \approx 1/(\tau_K\sqrt{N})$. This condition is equivalent to a dramatic reduction of the standard deviation of the measurement for each successive estimation step: $\bar{\Delta}_K \ll \bar{\Delta}_{K-1} \ll \dots \ll \bar{\Delta}_1$. This ensures that in each estimation step (say, the k -th step), the standard deviation of the estimation, $\Delta_k \approx \bar{\Delta}_k \approx 1/(\tau_k\sqrt{N})$, is dominated by the standard deviation $\bar{\Delta}_k$ of the measurement instead of the standard deviation $\Delta_{k-1} \approx \Delta_{k-1}$.

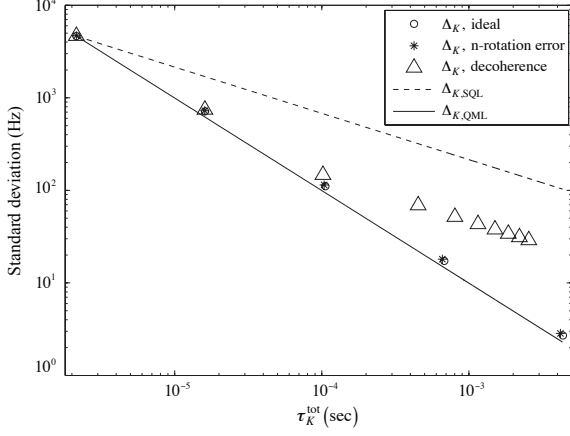


FIG. 5. Comparison of the standard deviation Δ_K of our protocol with the QML limit $\Delta_{K,QML}$ (solid line) and the SQL limit $\Delta_{K,SQL}$ (dashed line). How to choose τ_k is explained in the main text.

of the prior knowledge [cf. Eq. (10b)]. The condition $\tau_K \gg \tau_{K-1} \gg \dots \gg \tau_1$ is also equivalent to

$$\Delta_{k-1} \tau_k \gg \zeta, \quad (13)$$

since $\Delta_{k-1} \tau_k \approx \bar{\Delta}_{k-1} \tau_k = (\tau_k / \tau_{k-1}) \zeta$.

- For $\tau_1 = \tau_2 = \dots = \tau_K$, the precision $1/\Delta_K^2 = NK\tau_1^2$ coincides with the SQL precision $1/\Delta_{K,SQL}^2$ since in this case our protocol reduces to simple repetition of the same quantum circuit $M(\tau_1)$.

Then we give the best choice $\{\tau_k^{\text{ideal}}\}$ satisfying the QML condition Eq. (13) for the ideal case according to the description in Sec. IV B. We choose $\{\tau_k^{\text{ideal}}\}$ by taking the largest m_k such that $\Delta_{k-1} \tau_k \approx c$ at every step, where c is a constant satisfying $c \gg \zeta$ and $c^3 \ll 6\zeta$. Then $\{\tau_k^{\text{ideal}}\}$ automatically satisfies the QML condition Eq. (13) and the linear expansion condition Eq. (9b). From $\Delta_{k-1} \tau_k \approx c$, we have $\Delta_k \approx \bar{\Delta}_k \approx (\zeta/c)^k \Delta_0$, i.e., the standard deviation $\Delta_k \approx \bar{\Delta}_k$ is dramatically reduced by each successive estimation step. We also have $\tau_k^{\text{ideal}} \approx (c/\zeta)^k \tau_0$ (with τ_0 defined through $\Delta_0 \equiv \zeta/\tau_0$), i.e., an exponential increase of τ_k^{ideal} with k . Note that, for $B = 0.2$ T, we have $O(\eta^2) \sim 10^{-6}$. Therefore ζ can be as small as $\sim 10^{-5}$.

Finally we provide a numerical simulation for the estimation process. The parameters for the simulation are $A = 3.06$ MHz, $B = 0.2$ T, $N = 1000$, corresponding to $\zeta \approx 0.03$. We take $c = 0.2$, which satisfies $c \gg \zeta$ and $c^3 \ll 6\zeta$. The prior knowledge is $A_0 = 3.03$ MHz with a standard deviation $\Delta_0 = 0.03$ MHz, which has been reported by a previous experiment.¹⁷ Each controlled nuclear spin π rotation uses a 1- μ s square pulse with the Rabi frequency $\Omega = 500$ kHz. The electron spin rotations are regarded as instantaneous, as mentioned at the end of Sec. IV A. In Fig. 5, the proximity of Δ_K (circles) to $\Delta_{K,QML}$ (solid line) confirms the QML scaling of the estimation.

D. Realistic case: surpassing standard quantum limit

In this subsection, we take into account the nuclear spin rotation error and electron spin decoherence and discuss the optimal choice of $\{\tau_k\}$ and the resulting precision

$$\frac{1}{\Delta_K^2} = N \sum_{k=1}^K [Q(\tau_k) \tau_k]^2$$

of the estimation, derived from Eq. (7b) and (10b):

- Nuclear spin rotation error $Q(\tau) = 1 - \varepsilon^2 \equiv Q$. This error is equivalent to an increase of ζ to $\tilde{\zeta} \equiv \zeta/Q$. Then QML condition Eq. (13) becomes $\Delta_{k-1} \tau_k \gg \tilde{\zeta}$. For a general Q that is not too small (i.e., $1 \geq Q \gg \zeta$), the conclusion in the ideal case remains valid with $\zeta \rightarrow \tilde{\zeta}$, i.e., $\{\tau_k\}$ is chosen as $\tau_k \approx (c/\tilde{\zeta})^k (\tau_0/Q)$, where c is a constant subjected to $c \gg \tilde{\Delta}_Z$ and $c^3 \ll 6\tilde{\Delta}_Z$. In the simulation, we consider a typical error $\varepsilon = 0.1$ (corresponding to $\sim 3\%$ error in the rotation angle). Then we have $Q \approx 1$, and this allows us to set $c = 0.2$, the same value with the ideal case. As a result, we can choose $\tau_k \approx \tau_k^{\text{ideal}}$ and Δ_K is nearly the same as the ideal case. Therefore, the QML scaling is preserved for the realistic nuclear spin rotation error, as confirmed by the nearly complete coincidence between Δ_K (stars) and $\Delta_{K,QML}$ (solid line) in Fig. 5.

- Electron spin decoherence $Q(\tau) = e^{-2\tau/T_2^e}$. According to Sec. IV B, we should choose τ_k to maximize $Q(\tau_k) \tau_k$, subjected to the constraints in Eqs. (9). We use $\Delta_{k-1} \tau_k \approx c = 0.2$ in the simulation. In the presence of the electron spin decoherence, $Q(\tau)$ decreases as τ increases. Thus the QML condition $c \gg \zeta/Q(\tau_k)$ is no longer valid at some point. This is why Δ_k starts to deviate from the QML line at $k = 3$ in Fig. 5. Note that the estimation of $k = 3$ still surpasses the SQL. The maximum of $Q(\tau) \tau$ occurs at $\tau = T_2^e/2$, meaning that the standard deviation $\bar{\Delta}_k$ of the quantum circuit $M(\tau_k)$ is the smallest when $\tau_k \approx T_2^e/2$. Further increase of τ_k makes the precision of $M(\tau_k)$ worse. Once τ_k reaches $\tau_k \approx T_2^e/2$ at $k = k_c$, the estimation for $k > k_c$ is performed with $\tau_k = \tau_{k_c}$. Therefore, for $K = k_c + \tilde{K}$, further estimation steps beyond k_c (i.e., $k = k_c + 1, \dots, k_c + \tilde{K}$) increases the precision $1/\Delta_K^2$ by the SQL trend:

$$\frac{1}{\Delta_{k_c+\tilde{K}}^2} - \frac{1}{\Delta_{k_c}^2} \approx N \tilde{K} (T_2^e/2)^2.$$

For $T_2^e = 350 \mu\text{s}$, we have $k_c = 4$. Fig. 5 shows that Δ_K surpasses the SQL for $K < 4$, while it decreases parallel to the SQL for $K \geq 4$.

V. CONCLUSIONS

We have proposed an efficient quantum measurement protocol to estimate the hyperfine interaction between the electron

spin and the ^{15}N nuclear spin in the NV center. The essential idea of our protocol is the combination of the DQC1 parameter estimation¹¹ with the spin-echo technique. The spin echo eliminates the independent dynamics of the electron spin and the nuclear spin in the DQC1 model, but keeps the dynamics due to their interactions, whose strength is to be estimated. This protocol does not require the preparation of the nuclear spin state. We quantify the resources R as the total duration $\sum \tau$ of the estimation process. In the absence of any errors, the precision $1/\Delta^2$ (with Δ being the standard deviation) of the estimation approaches the quantum metrology limit (QML) $1/\Delta_{\text{QML}}^2 = O(R^2)$. This QML scaling is robust against the typical nuclear spin rotation error in realistic experimental conditions. In the presence of electron spin decoherence, the precision $1/\Delta^2$ keeps its QML scaling when $\tau \ll T_2^e/2$. Once τ becomes close to T_2^e further estimation steps increase the precision $1/\Delta^2$ according to the scaling $1/\Delta_{\text{SQL}}^2 = O(R)$ of the standard quantum limit (SQL). Due to the QML scaling in the initial stage, the overall precision still surpasses the SQL. We expect that this method can be applied to other solid state systems such as quantum dots or cold atoms to measure the interaction between two spins.

ACKNOWLEDGMENTS

This research was supported by the U. S. Army Research Office under contract number ARO-MURI W911NF-08-2-0032. The authors are grateful to David M. Toyli and Jiangfeng Du for helpful discussions.

Appendix A: Accounting for finite duration of controlled nuclear spin rotation

In this section, we assume that each of the two controlled nuclear spin π rotation in the quantum protocol (Fig. 4) is driven by a square π pulse with a duration $\tau_n \sim 1 \mu\text{s}$ and prove that inclusion of this finite duration amounts to a trivial

renormalization $\tau \rightarrow \tau + \tau_n$ in Eq. (5).

In Fig. 4, the initial state $\hat{\rho}_{\text{initial}} = |+\rangle\langle+| \otimes \hat{\rho}_n$ is prepared at $t = -\tau - \tau_n$. The first free evolution $e^{-i\hat{H}\tau}$ occurs during $t \in [-\tau - \tau_n, -\tau_n]$, followed by a controlled nuclear spin π rotation during $t \in [-\tau_n, 0]$. A fast electron spin π rotation is applied at $t = 0$, another controlled nuclear spin π rotation during $t \in [0, \tau_n]$, and another free evolution $e^{-i\hat{H}\tau}$ during $t \in [\tau_n, \tau + \tau_n]$.

First we calculate the evolution operator driven by a square π pulse applied during $t \in [t_1, t_2]$, with a central frequency $\omega = A - g_N\mu_N B - \delta$ (where $+\delta$ is the energy correction to $|1, \uparrow\rangle$ by the off-diagonal hyperfine interaction) resonant with the transition $|1, \uparrow\rangle \rightarrow |1, \downarrow\rangle$. During this pulse, the Hamiltonian $\hat{H}(t) = \hat{H} + \hat{V}(t)$ of the electron-nuclear spin qubits acquires an additional term

$$\hat{V}(t) = \frac{i\Omega_R}{2}(e^{-i\omega t}|1, \downarrow\rangle\langle 1, \uparrow| - e^{i\omega t}|1, \uparrow\rangle\langle 1, \downarrow|),$$

with a constant Rabi frequency $\Omega_R = \pi/(t_2 - t_1)$. With the aid of the interaction picture $|\Psi_I(t)\rangle \equiv e^{i\hat{H}t}|\Psi(t)\rangle$, the evolution operator $\hat{U}_V(t_2, t_1)$ during $t \in [t_1, t_2]$ can be calculated straightforwardly as $\hat{U}_V(t_2, t_1) = e^{-i\hat{H}t_2}e^{-i\hat{H}_I(t_2-t_1)}e^{i\hat{H}t_1}$, where $\hat{H}_I(t) \equiv e^{i\hat{H}t}\hat{V}(t)e^{-i\hat{H}t}$. Similar to the discussions in Sec. II B, we have $\hat{H}_I(t) = (\Omega_R/2)|1\rangle\langle 1| \otimes \hat{\sigma}_y + O(\Omega_R\eta)$, where $\eta \sim 10^{-3}$ for the external magnetic field $B = 0.2 \text{ T}$ used in our estimation. Therefore, the evolution $e^{-i\hat{H}_I(t_2-t_1)} \approx \hat{R}_y^n(\pi)$ coincides with the instantaneous controlled rotation and hence

$$\hat{U}_V(t_2, t_1) = e^{-i\hat{H}t_2}\hat{R}_y^n(\pi)e^{i\hat{H}t_1}.$$

With the aid of this result, it can be readily checked that the evolution operator for the composite evolution (as enclosed by the dashed box) in Fig. 4 is equal to $\hat{U}_{\text{com}}|_{\tau \rightarrow (\tau + \tau_n)}$. Therefore, inclusion of the finite duration τ_n of the controlled nuclear spin rotation amounts to replacing τ with $(\tau + \tau_n)$ in Eq. (5). Note that the nuclear spin relaxation time and decoherence time $\gtrsim 1 \text{ ms}$ are much longer than $\tau_n \sim 1 \mu\text{s}$ and hence have negligible influence on this result.^{2,3}

* Current address: Beijing Computational Science Research Center, Beijing 100084, China

¹ T. Gaebel, M. Domhan, I. Popa, C. Wittmann, P. Neumann, F. Jelezko, J. R. Rabreau, N. Stavrias, A. D. Greentree, S. Praver, J. Meijer, J. Twamley, P. R. Hemmer, and J. Wrachtrup, *Nature Phys.* **2**, 408 (2006).

² P. Neumann, J. Beck, M. Steiner, F. Rempp, H. Fedder, P. Hemmer, J. Wrachtrup, and F. Jelezko, *Science* **329**, 542 (2010).

³ G. D. Fuchs, G. Burkard, P. V. Klimov, and D. D. Awschalom, *Nature Phys.* **7**, 789 (2011).

⁴ L. Childress, M. V. Gurudev Dutt, J. M. Taylor, A. S. Zibrov, F. Jelezko, J. Wrachtrup, P. R. Hemmer, and M. D. Lukin, *Science* **314**, 281 (2006).

⁵ P. Neumann, N. Mizuchi, F. Rempp, P. Hemmer, H. Watanabe, S. Yamasaki, V. Jacques, T. Gaebel, F. Jelezko, and J. Wrachtrup, *Science* **320**, 1326 (2008).

⁶ V. Giovannetti, S. Lloyd, and L. Maccone,

Science **306**, 1330 (2004).

⁷ V. Giovannetti, S. Lloyd, and L. Maccone, *Phys. Rev. Lett.* **96**, 010401 (2006).

⁸ J. A. Dunningham, *Contemp. Phys.* **47**, 257 (2006).

⁹ J. P. Dowling, *Contemp. Phys.* **49**, 125 (2008).

¹⁰ G. Goldstein, P. Cappellaro, J. R. Maze, J. S. Hodges, L. Jiang, A. S. Sørensen, and M. D. Lukin, *Phys. Rev. Lett.* **106**, 140502 (2011).

¹¹ S. Boixo and R. D. Somma, *Phys. Rev. A* **77**, 052320 (2008).

¹² E. Knill and R. Laflamme, *Phys. Rev. Lett.* **81**, 5672 (1998).

¹³ A. Datta, A. Shaji, and C. M. Caves, *Phys. Rev. Lett.* **100**, 050502 (2008).

¹⁴ B. P. Lanyon, M. Barbieri, M. P. Almeida, and A. G. White, *Phys. Rev. Lett.* **101**, 200501 (2008).

¹⁵ W. Yang, Z. Y. Wang, and R. B. Liu, *Frontiers of Physics* **6**, 2 (2011).

¹⁶ V. Jacques, P. Neumann, J. Beck, M. Markham, D. Twitchen,

- J. Meijer, F. Kaiser, G. Balasubramanian, F. Jelezko, and J. Wrachtrup, *Phys. Rev. Lett.* **102**, 057403 (2009).
- ¹⁷ S. Felton, A. M. Edmonds, M. E. Newton, P. M. Martineau, D. Fisher, D. J. Twitchen, and J. M. Baker, *Phys. Rev. B* **79**, 075203 (2009).
- ¹⁸ J. Harrison, M. J. Sellars, and N. B. Manson, *J. Lumin.* **107**, 245 (2004).
- ¹⁹ B. B. Buckley, G. D. Fuchs, L. C. Bassett, and D. D. Awschalom, *Science* **330**, 1212 (2010).
- ²⁰ G. D. Fuchs, V. V. Dobrovitski, D. M. Toyli, F. J. Heremans, and D. D. Awschalom, *Science* **325**, 1520 (2009).
- ²¹ G. D. Fuchs, V. V. Dobrovitski, D. M. Toyli, F. J. Heremans, C. D. Weis, T. Schenkel, and D. D. Awschalom, *Nature Phys.* **6**, 668 (2010).
- ²² G. Balasubramanian, P. Neumann, D. Twitchen, M. Markham, R. Kolesov, N. Mizuochi, J. Isoya, J. Achard, J. Beck, J. Tissler, V. Jacques, P. R. Hemmer, F. Jelezko, and J. Wrachtrup, *Nature Mater.* **8**, 383 (2009).
- ²³ B. Naydenov, F. Dolde, L. T. Hall, C. Shin, H. Fedder, L. C. L. Hollenberg, F. Jelezko, and J. Wrachtrup, *Phys. Rev. B* **83**, 081201 (2011).